Landscape Ecol
https://doi.org/10.1007/s10980-020-01084-8

RESEARCH ARTICLE

Characterizing three dimensional (3-D) morphology of residential buildings by landscape metrics

Yupeng Liu · Chong Chen · Jiajia Li · Wei-Qiang Chen

Received: 19 December 2019 / Accepted: 28 July 2020

Abstract
Context The key attributes of landscape pattern include composition and configuration, which can be depicted by landscape/spatial metrics. An emerging pathway is leveraging vertical data to advance three-dimensional (3-D) spatial metrics to interpret landscape attributes and quantify 3-D patterns.
Objectives We introduced a suite of spatial metrics to recognize 3-D morphological characteristics of residential communities and examine their temporal changes.
Methods Seventeen 3-D spatial metrics were designed and computed at patch-, class-, and landscape-levels based on building footprints and height information in geographic information system (GIS). These metrics characterized 3-D forms of residential communities, including number, area, height, shape, and diversity. These 3-D features were further used to recognize five typical built types based on the scheme of local climate zone (LCZ) and quantify their 3-D morphological changes with rapid urbanization.
Results The 3-D spatial metrics performed well in describing vertical and volumetric characteristics of residential communities and distinguishing five typical built types in Xiamen, China. Our results indicated that architectural styles of residential communities changed from homo- to mixed-rise buildings and from compact to open arrangement with rapid urbanization.
Conclusions Both 2-D and 3-D features are key attributes of the landscape. Our results showed that 3-D spatial metrics were not only useful tools for quantifying surface patterns but also key complements to vertical feature characterization, offering advantages in representing urbanization over the existing indexes. Growing 3-D datasets have great potential to develop more valuable metrics for characterizing spatial features, capturing ecological processes, and understanding drivers in various landscape contexts.

Keywords Urban form · Spatial pattern · Spatial metric · Local climate zones (LCZs) · Remote sensing · Urban sustainability ·

Y. Liu · J. Li · W.-Q. Chen
Key Lab of Urban Environment and Health, Institute of Urban Environment, Chinese Academy of Sciences, Xiamen 361021, Fujian, People's Republic of China

Y. Liu · J. Li · W.-Q. Chen (✉)
Xiamen Key Lab of Urban Metabolism, No. 1799 Jimei Road, Xiamen 361021, Fujian, People's Republic of China
e-mail: wqchen@iue.ac.cn

C. Chen
Urban-Rural Planning Administration Center, Ministry of Housing and Urban-Rural Development (MOHURD), Beijing, People's Republic of China

J. Li · W.-Q. Chen
University of Chinese Academy of Sciences, 100049 Beijing, People's Republic of China

Published online: 06 August 2020

High-resolution urban grids (HUGs) · Industrial ecology

Introduction

Landscape metrics can describe spatiotemporal patterns of natural and artificial environments through counting patch number and size, depicting shape complexity, measuring relative richness and diversity, and quantifying aggregation and contagion (O'Neill et al. 1988). These metrics contain highly condensed information of landscape composition and configuration and are central to patch-mosaic model (Forman 1995) and hierarchical patch dynamics (HPD) paradigm (Wu and Levin 1994, 1997; Wu and David 2002). Traditional landscape metrics were widely used to quantify two-dimensional (2-D) spatiotemporal patterns based on land use/cover data (Costanza et al. 2019). For example, they performed well in characterizing habitat fragmentation (Bailey 2011), urban expansion/shrink (Luck and Wu 2002; Wu et al. 2011; Li et al. 2013a, b; Reis et al. 2016), and other environmental processes (Zurlini et al. 2006). Furthermore, they could be used to interpret the effects of landscape elements on environmental and social processes (Turner 2005), such as biodiversity loss (Fahrig 2003; Turner et al. 2003), runoff erosion (Ludwig et al. 2005), air pollution (Bechle et al. 2011; Bereitschaft and Debbage 2013; Liu et al. 2017a, b, 2018a, b, c), urban sprawl (Galster et al. 2001; Ewing et al. 2002; Tsai 2005), urban heat island (UHI) (Tian et al. 2019), energy use (Ewing and Rong 2008), and transportation facility (Ewing et al. 2003). A better understanding of the relationship between spatial pattern and socio-ecological processes by landscape metrics is important to increase landscape resilience (Peterson 2002; Cumming 2011), improve ecosystem services (Costanza et al. 1997; Metzger et al. 2006; Termorshuizen and Opdam 2009; Frank et al. 2012; Hao et al. 2017; Yu et al. 2019), and promote sustainability and human well-being (Wu 2013).

A new emerging pathway is leveraging vertical information in the landscape to advance three-dimensional (3-D) spatial pattern analysis based on new data sources (Chen et al. 2014; Davis et al. 2016; Liu et al. 2017a, b; Wu et al. 2017; Kedron et al. 2019). One of the sources is to establish discrete building footprints in geographic information system (GIS) and collect height information based on social-media big data. For example, the Open Street Map (OSM) is a digital map database through crowd-sourced and volunteered geographic information of buildings and infrastructure around the world (https://www.openstreetmap.org/). All features of buildings and infrastructure are open to editing by any member of the user community. Another important source is to create 3-D images of landscapes based on contin uous grid data from remote sensing instruments, such as aerial photography, Synthetic Aperture Radar (SAR), or Light Detection and Ranging (LiDAR). For example, the shadow length of objects recorded by aerial images can be used to retrieve height information based on the relationship with local elevation and zenith angle of the monitor and sun (Liu et al. 2017a, b). SAR data can map 3-D positions of objects based on the time difference between the transmission and reception of electromagnetic waves (Che et al. 2018). LiDAR data represent landscapes through 3-D point clouds of objects (Che et al. 2018).

However, traditional landscape metrics can not be directly adapted to 3-D pattern analysis (e.g., through Fragstats) due to additional vertical information. Therefore, developing 3-D spatial metrics offers a new approach and may shed light on the quantification of landscape 3-D patterns. Only a few studies have been conducted with landscape metrics in characterizing 3-D gradient surface (Wu et al. 2017), identifying urban 3-D characteristics (Liu et al. 2017a, b), and assessing urban 3-D form changes after a disturbance (Kedron et al. 2019). These 3-D characteristics of vegetation and buildings have been further used to assess environmental impacts, primarily on urban heat island (Davis et al. 2016; Zhang et al. 2017; Tian et al. 2019).

There is a growing interest in integrating two fields of 3-D form characterization and urban heat island. For example, the "local climate zone" (LCZ), as a standard classification system, provides an objective protocol for measuring the magnitude of the urban heat island effect in any city by describing physical and morphological characteristics of a local site based on ten quantitative metrics (Stewart and Oke 2012). The majority of these metrics describe surface cover properties (e.g., albedo, admittance) and 2-D geometry (e.g., impervious surface fraction) and minority depict 3-D morphology (e.g., height) (Stewart and Oke 2012).

To further advance this integration of the LCZ scheme with landscape metrics (especially on 3-D morphological metrics), this study (1) Kedron et al. (2019) based on gradient raster dataset from remotely sensed images. Another important purposes of new metrics design is to guarantee these metrics are meaningful and interpretable across various landscape contexts and to apply them into dynamic analysis on urban environment (Kedron et al. 2019). We hereby (2) identified typical residential communities based on LCZs and characterized their features by both 2-D and 3-D spatial metrics and (3) uncovered morphological changes of built environment at community (or patch)-, LCZ (or class)-, and landscape-levels in a city under rapid urbanization.

Data and methods

Assumptions on the morphological quantification of residential communities

In Chinese cities, residential community is the basic unit of organization for housing residents. A residential community usually spans thousands of meters to a few kilometers in land surface, contains one or more buildings in the contiguous locality within a clear boundary (usually surrounded by walls or fences), and houses hundreds to thousands of families under the same management company or neighborhood committee. Both the spatial extent and heterogeneous composition of residential community match with the definition of "local climatic zones (LCZs)" (Stewart and Oke 2012). We identified five classic types of residential communities (built type I~IV) in Chinese cities and matched them with LCZs categories (Fig. 1). The built type I~IV were directly related to standard LCZ classes 3~6 in Stewart and Oke 2012, respectively. The built type V was related to the subclass of LCZ 6_4 based on local architectural culture, which designed both low-rise villas and high-rise skyscrapers in the same community (Fig. 1). The difference with standard LCZ classes was that we set 11 and 8 floors as thresholds to distinguish high-, medium-, and low-rise buildings and designed several new spatial metrics to characterize their 2-D and 3-D morphology (Fig. 1).

2-D and 3-D spatial metrics

Traditional patch-based spatial metrics were defined on four organizational levels: cells, patches, classes, and landscapes (McGarigal et al. 2012). In this study, we defined the "cells" (the finest level) as individual buildings and "patches" as residential communities (Fig. 1). Five built types based on LCZs were defined as "classes" and every community belonged to one of them (Fig. 1). The landscape-level referred to the city and therefore included all buildings and communities (Fig. 1).

We introduced a suite of 5 categories and a total of 17 spatial metrics to characterize both 2-D and 3-D morphological features of urban residences at the cell-, patch-, class-, and landscape-levels (Tables 1 and 2). Five categories contained information on number, area, height, shape, and diversity aspects (Table 2). Number-related metrics included the total number and density of buildings at the patch-, class-, and landscape-levels (Tables 1 and 2). Area-related metrics included the total areas of building footprints, open space, and communities and the proportion of paved surface at the patch-, class-, and landscape-levels (Tables 1 and 2). A normalized perimeter/area ratio was selected to quantify the shape complexity of buildings (Tables 1 and 2). Shannon's diversity index was used to measure the diversity of classes (built types) in the landscape (Tables 1 and 2). Height-related metrics included the height of individual building (=floor $\times$ 3 m), area-weighted height of buildings, and height variation at the patch-, class-, and landscape-levels (Tables 1 and 2). Rather than arithmetic average of building height, the area-weighted height was an updated metric for indicating the 'average' height of several buildings and considering the footprint area of these buildings as weights. Based on building footprints and heights, total building volumes and the plot ratio of every community were calculated and the class with the largest building volume was identified (Tables 1 and 2). These spatial metrics were used to characterize features of five built types of residential communities and uncover morphological changes of built environment from 1990 to 2018 in Xiamen, China.

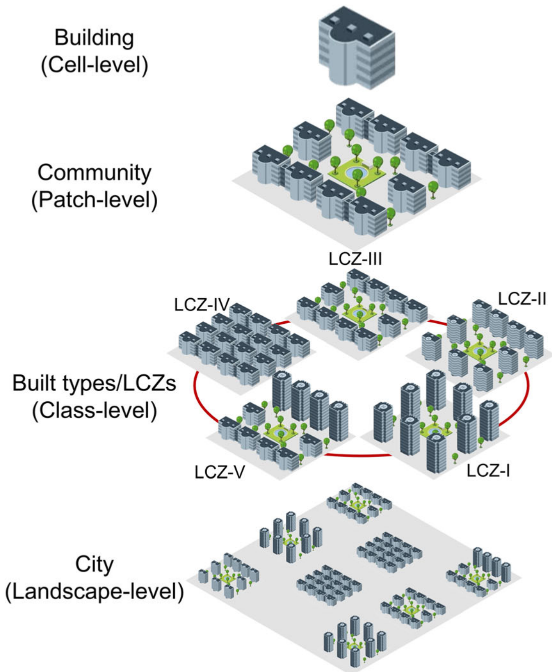

Built types (LCZs)	Description (Stewart & Oke 2012)	Height	PLAND_2D	Plot ratio	Height variation
I Open high-rise 	Open arrangement and medium density of tall buildings built by concrete and steel. Some trees.	>11 floors	Medium	High	Low
II Open mid-rise 	Open arrangement and medium density of med-rise buildings built by concrete and steel. Some trees.	8~11 floors	Medium	Medium	Low
III Open low-rise 	Open arrangement and medium density of low-rise buildings built by brick, concrete and steel. Some trees.	<8 floors	Medium	Medium	Low
IV Compact low-rise 	Dense mix of low-rise buildings built by brick, concrete and steel. Few or no trees.	<8 floors	High	Medium	Low
V Open mix-rise 	Open arrangement and medium density of mix-rise buildings built by brick, concrete and steel. Some trees.	2~50 floors	Medium	Medium	High

Fig. 1 Assumptions on the morphology of typical residential communities. (adapted from Stewart and Oke 2012) in Xiamen, China

Data on residential buildings in Xiamen, China

We digitalized both footprints of individual buildings and boundaries of residential communities as vector polygons from both historical atlases and commercial companies (e.g., Google Earth, Baidu Map) (Fig. 2). A unified attribute table was created for recording attribute information (e.g., floor number, vintage), which collected from real estate agencies (e.g., Lianjia, Soufun). Among them, the floor number was recorded into the attribute table for only building polygons and vintage information was recorded into the attribute table for both building and residential community polygons. Field surveys were conducted between March 2018 and October 2019 for data filling and cleaning, especially for missing values of the building footprints, floor numbers in newly built communities and vintage information for the buildings with a long history (e.g., earlier than 1980 s). Non-residential buildings, such as industrial, commercial, and public buildings, were not included in this analysis due to data availability. In contrast to systematic records of the built-up year for residential buildings, it is difficult to find systematic records of vintage information for non-residential buildings from government documents, commercial reports, online or field surveys. Besides, it is also hard to estimate building height accurately for non-residential buildings due to a very high uncertainty on height range per floor (3.9~6.4 m) according to Chinese construction standard, which compared to residential buildings' (2.6~3.2 m).

Results

Applying 3-D metrics to distinguish five classic types of residential communities in Xiamen based on morphological features

Morphological features of five classic types of residential communities in Xiamen were characterized by a suite of 3-D landscape metrics (Fig. 3). The compact communities (Type IV) could be identified first because they owned a relatively higher percentage of paved landscape (PLAND_2D) than those values in the open space communities (Type I, II, III, and V) (Fig. 3a). The values of the percentage of paved landscape (PLAND_2D) in the compact

Table 1 Descriptions of selected landscape metrics in this study

Landscape metric[a]	Abbre.	Unit	Equation	Description
Number of buildings	NB	–	$\sum_{i \in j\|k\|l} n_i$	The number of buildings $n_{i=1,2,\ldots}$ was counted in the community j, class k, or landscape l
Community area	CA	m^2	$\sum_{j \in k\|l} A_j$	Where A is the total footprint area of the community j in the class k or landscape l
Building density	BD	#/	m^2	$\frac{NB_{j\|k\|l}}{CA_{j\|k\|l}}$
Where NB is the total number of buildings of the community j, class k, or landscape l and CA is total footprint area of the community j, class k, or landscape l				
Building footprint area	BA	m^2	$\sum_{i \in j\|k\|l} a_i$	Where a is the footprint area of an individual building i in the community j, class k, or landscape l
Open space area	OSA	m^2	$CA_{j\|k\|l} - BA_{j\|k\|l}$	Where BA is the total footprint area of buildings and CA is the total footprint area of the community j, class k, or landscape l
Percentage of landscape paved by buildings	PLAND_2D	%	$\frac{BA_{j\|k\|l}}{CA_{j\|k\|l}}$	Where BA is the total footprint area of buildings in the community j, class k, or landscape l and CA is footprint area of the community j, class k, or landscape l
Height	H	m	$floor \times 3$	The floor of individual building is multiplied by 3 to convert to meters
Height variation	Var	m	$\sqrt{\frac{\sum_{i=1}^{n} (H_i - H_{mean})^2}{NB_{j\|k\|l}}}$	Where H_i is the height of individual building i, H_{mean} is the average value of building height in community j, class k, or landscape l, and NB is the total number of buildings in the community j, class k, or landscape l
Total floor area	TFA	m^2	$\sum_{\substack{i=1 \\ i \in j\|k\|l}}^{n} a_i \times floor_i$	Where a is the footprint area and *floor* is the number of levels of an individual building i in the community j, class k, or landscape l
Volume	Vol	m^3	$\sum_{\substack{i=1 \\ i \in j\|k\|l}}^{n} a_i \times H_i$	Where a is the footprint area of an individual building i in the community j, class k, or landscape l and H is the height (in meters) of an individual building i in the community j, class k, or landscape l
Area-weighted height	AWH	m	$\frac{Vol_{j\|k\|l}}{BA_{j\|k\|l}}$	The area-weighted height was the weighted mean height of buildings, where the weights are based on the total footprint area of buildings (BA) in the community j, class k, or landscape l
Plot ratio	PR	–	$\frac{TFA_{j\|k\|l}}{CA_{j\|k\|l}}$	Where TFA is the total floor area of buildings in the community j, class k, or landscape l and CA is total footprint area of the community j, class k, or landscape l
Percentage of build type in the landscape	PLAND_3D	%	$\frac{Vol_k}{\sum_{k=1}^{m}(Vol_k)} \times 100$	Where Vol is the building volume of the class k. The result is multiplied by 100 to convert to percentage
Largest class index	LCI	%	$\frac{\sum_{k=1}^{m} max(Vol_k)}{\sum_{k=1}^{m}(Vol_k)} \times 100$	Where $\max(Vol_k)$ is the building volume of the largest class k. The result is multiplied by 100 to convert to percentage.
Edge	E	m	$\sum_{\substack{i=1 \\ i \in j\|k\|l}}^{n} E_i$	Where E is the total length of edges of an individual building i in the community j, class k, or landscape l.
Landscape shape index	LSI	–	$\frac{0.25E_{i\|j\|k\|l}}{\sqrt{BA_{i\|j\|k\|l}}}$	Where E is the total length of edges and BA is total footprint area of an individual building i, community j, class k, or landscape l
Shannon's diversity index	SHDI	–	$-\sum_{k=1}^{m} P_k \ln P_k$	Where P is the proportion of class k in the landscape and the value of the proportion refers to $PLAND\_3D_k$

[a] Adapted from McGarigal et al. (2012)

communities ranged between 40 and 60%, which compared to the values varied between 20 and 40% in the open arrangement communities (Fig. 3a). From low-, mid-, to high-rise communities, the mean values of building heights (H) generally increased from ~20 m (Type III&IV), ~30 m (Type II), to ~60 m (Type I) (Fig. 3b). The plot ratio (PR) also increased with the building height due to more floor

Table 2 Three dimensional (3-D) spatial metrics

Categories	Landscape metrics[a]	Abbreviation	Unit	Building (cell-)	Community (patch-)	LCZ (class-)	City (Landscape-)
Number	Number of buildings	NB	–		✓	✓	✓
	Building density	BD	#/ m^2		✓	✓	✓
Area	Building footprint area	BA	m^2	✓	✓	✓	✓
	Open space area	OSA	m^2		✓	✓	✓
	Community area	CA	m^2		✓	✓	✓
	Percentage of landscape paved by buildings	PLAND_2D	%		✓	✓	✓
3-D	Height	H	m	✓			
	Area-weighted height	AWH	m		✓	✓	✓
	Height variation	Var	m		✓	✓	✓
	Total floor area	TFA	m^2	✓	✓	✓	✓
	Volume	Vol	m^3	✓	✓	✓	✓
	Plot ratio	PR	–		✓	✓	✓
	Percentage of building volume in the landscape	PLAND_3D	%				✓
	Largest class index	LCI	%				✓
Shape	Edge	E	m	✓	✓	✓	✓
	Landscape shape index	LSI	–	✓	✓	✓	✓
Diversity	Shannon's diversity index	SHDI	–				✓

[a] Adapted from McGarigal et al. (2012)

area (TFA) could be provided by taller buildings (Fig. 3c). Finally, the mix-rise communities (Type V) showed more variation in building heights (Var, 9~1 m) than the other four types of communities (0~6 m) (Fig. 3d).

Applying 3-D metrics to quantify morphological changes of residential buildings during urbanization

During 1990–2018, morphologies of residential communities in Xiamen evolved from the compact low-rise type to mix with open mid- and high-rise types (Figs. 4, 5a). In the 1990 s, the compact communities dominated Xiamen's built type and led to high building density (BD) and the percentage of paved landscape (PLAND_2D) (Fig. 5b, c). After 1990 s, more open arrangement communities were built (Figs. 4, 5a), resulting in decreases in the building density (BD) from ~900 buildings/km^2 in 1990 to ~550 buildings/km^2 in 2018 (Fig. 5b) and the percentage of paved landscape (PLAND_2D) from ~40 to ~33% (Fig. 5c). Meanwhile, most of these open arrangement communities owned mid- and high-rise buildings which led to increases in area-weighted building height (AWH), volume (Vol), plot ratio (PR), and shape complexity (LSI) (Fig. 5b–d). At the city level (landscape-level), the largest class index (LCI) generally decreased from ~90% in 1990 to ~28% in 2018 (Fig. 5e). Among five types of residential communities, the largest one in Xiamen was the compact low-rise community (type IV) but its proportion (LCI) kept decreasing (Fig. 5e). After 2017, the total floor area (TFA) and volume (Vol) of the open high-rise communities (Type I) surpassed that value of the compact low-rise type (type IV), which led to the former became the dominative built type in Xiamen (Fig. 5a). The Shannon's diversity index (SHDI) also increased rapidly with the expansion of open arrangement communities after the 1990 s and saturated during 2010–2018 (Fig. 5e) due to a well-balanced mix of five residential types (Fig. 5a).

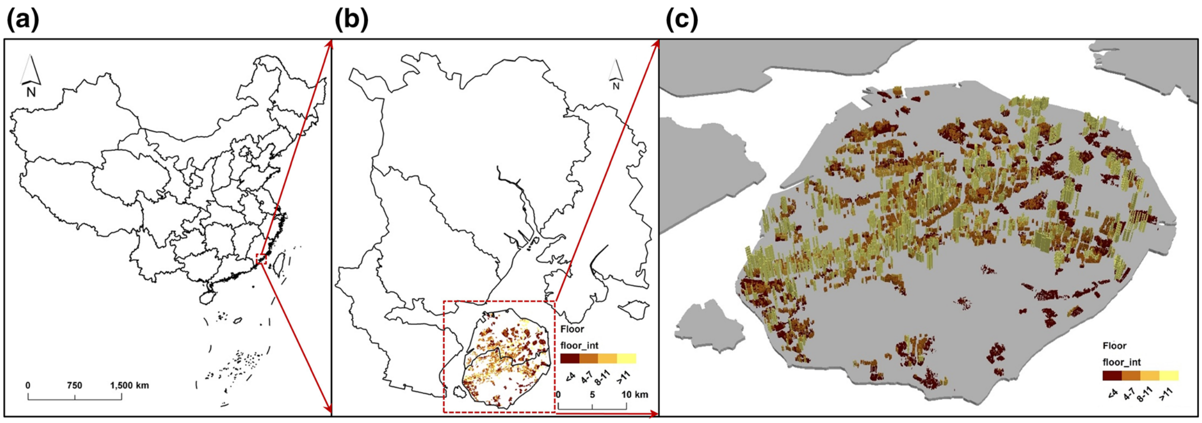

Fig. 2 The study area map of Xiamen, China. **a** The location of Xiamen in China. **b** The location of study area in Xiamen city. **c** Footprint and height information of residential buildings in the study area

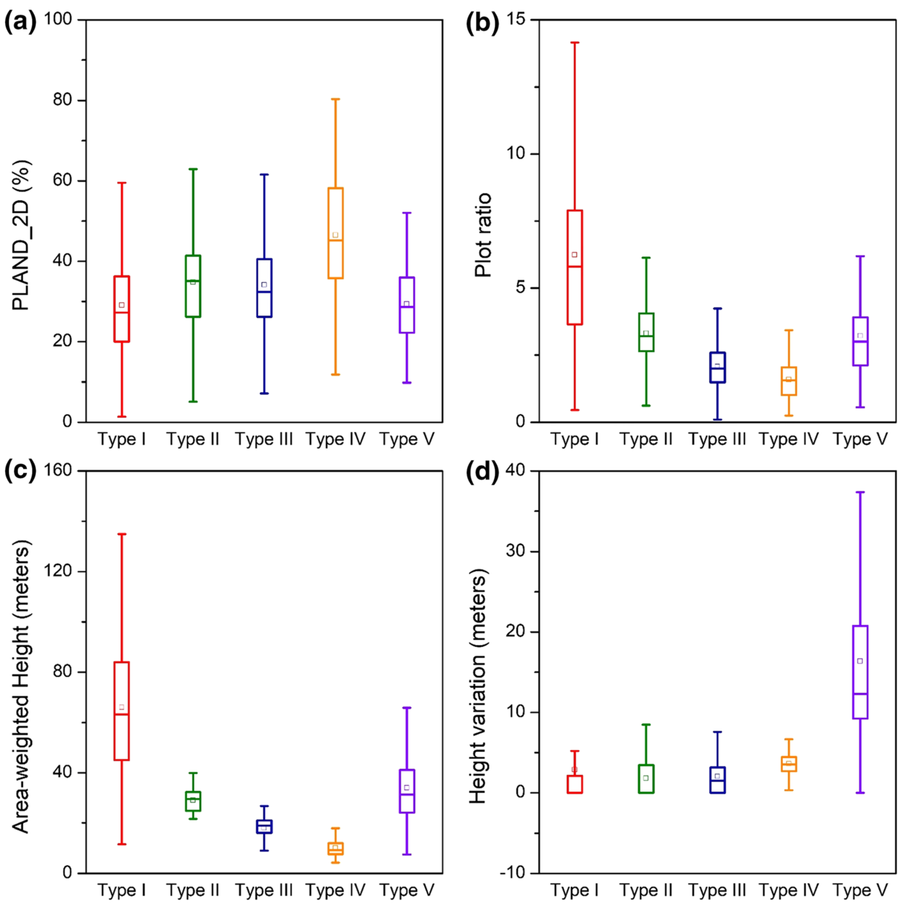

Fig. 3 Distinguishing morphological disparity of typical residential communities in Xiamen, China

Discussion

Extending the LCZs scheme and its applications by integrating 3-D form characteristics

Integrating with 3-D metrics successfully advances vertical and volumetric characterization of LCZs. Rather than existing metrics for LCZ classification, these new metrics help to describe five categories of composition and configuration information, including number, area, height, shape, and diversity on multiple organizational levels, from an individual building to the whole city (Table 2). Among them, buildings number and area metrics can measure the size and density of buildings and suggest the degree of interspersion or sprawl of the built-up area in a city. Moreover, the percentage of paved landscape (PLAND_2D) and open space area (OSA) are important factors that affect the ventilation of air pollution (Priyadarsini et al. 2008; Wong et al. 2010; Zhang et al. 2017). Landscape shape index (LSI) is a measure of the surface shape complexity of buildings or communities, which is related to lots of socioeconomic phenomena (Ewing et al. 2002; Bechle et al. 2011; Pauliuk and Müller 2014; Thacker et al. 2019). For example, a compact building tends to save energy rather than detached, dispersed houses (Ewing and Rong 2008). Existed communities with complex forms are easier to cause local traffic congestion and affect urban design and planning through the "lock-in" effect (Bechle et al. 2011). For height-related metrics, high-rise buildings lead to more

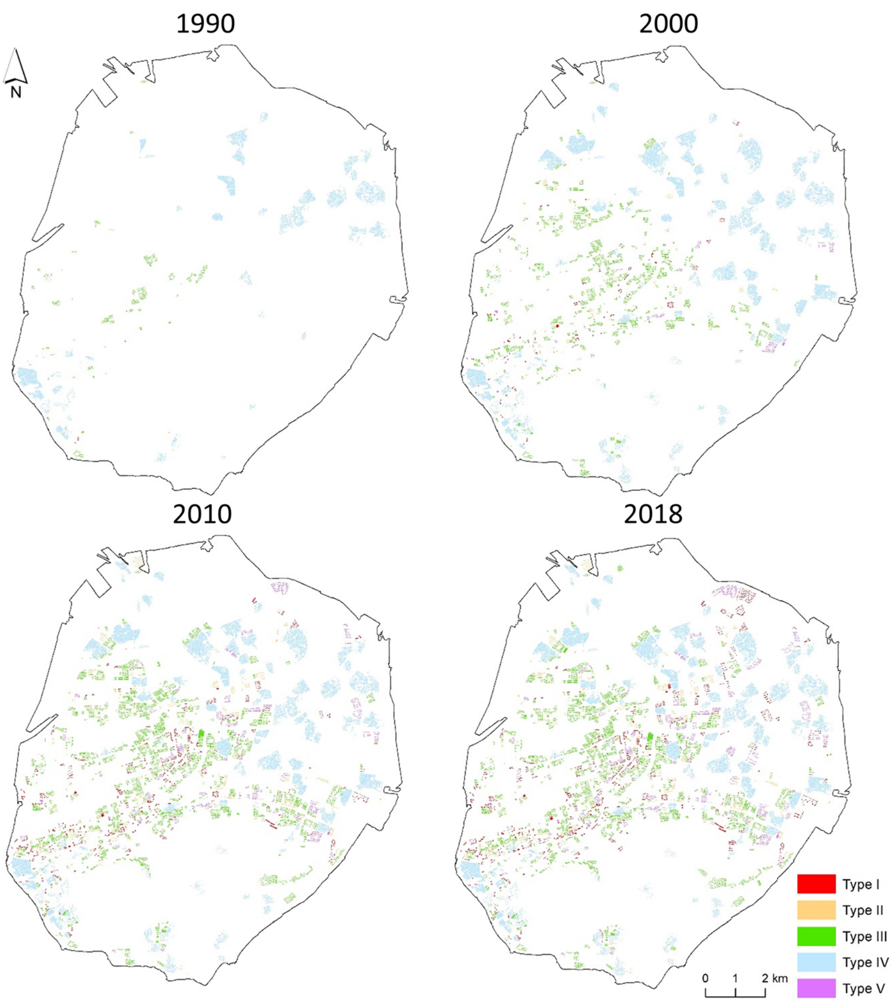

Fig. 4 Spatial patterns of residential communities in Xiamen, China

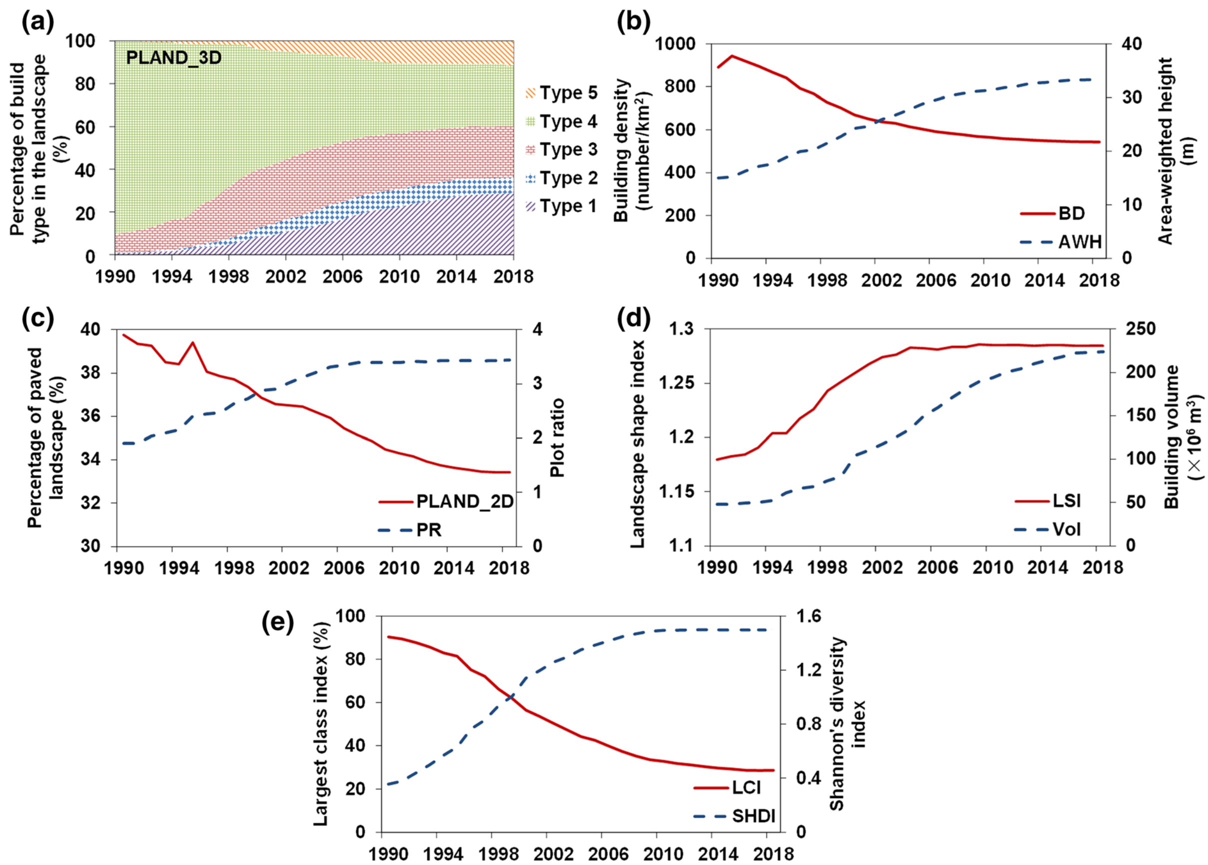

Fig. 5 Temporal changes of 3-D landscape metrics in Xiamen, China

demands on pollution-intensive construction materials (e.g., steel, cement) and thus have substantial environmental effects (Pauliuk and Müller 2014; Xi et al. 2016; Thacker et al. 2019). In use stage, high-rise buildings tend to consume more energy (2.5 times electricity per square meter of floor area) than low-rise buildings due to greater exposure to wind and sun, which might increase the need for heating and cooling (Zielinska-Dabkowska and Xavia 2019). Furthermore, the variation of building heights (Var) has been proven effective against air pollution by enhancing vertical convection (Hang et al. 2012; Yuan et al. 2014; Liu et al. 2018a, b, c). The plot ratio (PR) has been widely used to measure community livability and even affect the land prices (Zhang et al. 2018). At the landscape (city) level, the largest class index (LCI) indicates dominative built types or LCZs in a city and Shannon's diversity index is used to measure the degree of land-use mix. A low level of land-use mix usually leads to transportation-oriented design and planning of land use and affects social accessibility (Song and Knaap 2004). Overall, we believe that adding more 3-D morphological characteristics in LCZ scheme can not only give valuable information to understanding how could they affect UHI magnitude (Tian et al. 2019), but also extend more useful applications of LCZs, for example, in parameterization of climate modeling (Cao et al. 2020), urban planning guidance (Perera and Emmanuel 2018), and community livability assessment (Zielinska-Dabkowska and Xavia 2019).

Significant effects of the 3-D form change on urban environment and human health

The temporal changes of 3-D morphology in urban built environment uncovered in this study indicate that the evolution of built type and the improvement of the community livability under the rapid urbanization in Xiamen, China. More open space (OSA)

Fig. 6 Photos of three typical residential communities in Xiamen, China. **a** The compact low-rise community (Bashi/八市, built by 1930 s), **b** The open low-rise community (Jianxingxiaoqu/建兴小区, built by 1992). **c** The open high- (or mix-) rise community (Zhonghangcheng/中航城, built by 2015). Photo by Yupeng Liu

has been designed in new open arrangement communities (LCZ-I, II, III, and V), which can be used to arrange more available green space for recreation and leisure and hence makes communities be more environmentally friendly and livability (Fig. 6). Furthermore, light accessibility, as an important sustainable indicator for human physical health and mental well-being, significantly increases in open arrangement communities (Fig. 6). The improvement of light accessibility helps to keep human health against related diseases such as vitamin-D deficiency or short-sightedness (Zielinska-Dabkowska and Xavia 2019). Meanwhile, sunshine helps with cleaning air pollution by enhancing temperature gradient and vertical convection (Liu et al. 2018a, b, c). However, booming new high-rise buildings (LCZ-I and V) lead to vertical growth of city and leave enormous shadows on the ground and low-rise buildings. Overshadowing by tall buildings can weaken clean energy generation by photovoltaic solar panels on roofs, reduce light accessibility on low-level apartments, and limit the growth of vegetation on the ground (Zielinska-Dabkowska and Xavia 2019). These deficits need inter- even trans-disciplinary committees to provide improvement advice by not only experts and professionals from fields of urban planning, architecture, engineering, and medicine but also public and other stakeholders.

Advances and limitations

This study successfully merged GIS-based data on building footprint and social-media data on building height and vintage, and used them to examine urban 3-D morphological changes, which is a complement to previous studies based on gradient raster dataset derived from remotely sensed instruments (Wu et al. 2017; Che et al. 2018; Kedron et al. 2019). The certain building footprints in vector data reduce the uncertainty of boundary generated by the threshold of cut-points on gradient raster data. However, the vector data on building footprint and height have their own uncertainties. First, the building footprint is often the outer surfaces of roofs and not those of walls (Augiseau and Barles 2017), resulting in overestimations of surface area (BA) and building volume (Vol). Second, the building height (H) is estimated by the total floor number times the average height per floor (e.g., 3 m in this study) to convert to meters (Table 1). For the former parameter, the recorded floor number usually neglects the height of the roof and therefore leads to an underestimation of the total height of a building. For the latter parameter, the height for a single floor may vary among communities and vintages and thus add ± 10% error compared to reality. Moreover, we used the build-up year of buildings instead of multi-temporal data to analyze the temporal changes of urban built environment due to data availability. The missing data on old buildings (usually belong to LCZ-IV), especially for those have been demolished and replaced by new communities (usually belong to LCZ-I, II, and V), would lead to an underestimation of total number (NB), area (CA, BA, OSA), volume (TFA, Vol), and related proportion (LCI) in specific LCZs but have fewer impacts on average-based metrics (PLAND_2D, PR, AWH). Besides, the values of 3-D metrics at class (LCZ)- and landscape (city)-levels were based on the patch-level calculation. Changes in the definition of a patch, for example, from the irregular shape of a residential community (e.g., in China) to a rectangle block (e.g., in USA), would lead to the modifiable areal unit problem (MAUP). The advantages of choosing residential communities as patches include (1) the spatial extent of each community matches the definition of LCZ and (2) each individual community in Chinese cities is designed by the same construction company and thus has a unified architectural style and belongs to a certain LCZ.

Conclusions

Both 2-D and 3-D features are key attributes of a landscape. Our study has shown that 3-D spatial metrics can characterize both surface and vertical patterns of the urban built-up environments rather than traditional 2-D metrics. They performed well in describing the morphological characteristics of five typical residential communities based on LCZ scheme and recognizing the differences among them. They are also useful tools to characterize spatiotemporal changes in urban 3-D patterns. The application of these 3-D spatial metrics in the Xiamen case has successfully revealed the evolution of architectural styles in residential communities from homo- to mix-rise buildings and from compact to open arrangement. Changes in 3-D form of residential communities increase the brightness of apartments and the greenness of communities and finally improve their livability. Continuing advances in 3-D datasets are of great help to develop more various and valuable spatial metrics for better characterizing spatial features, capturing ecological processes, and understanding drivers in various landscape contexts.

Acknowledgements We thank the members of the Resources and Urban Sustainability group at the Institute of Urban Environment, Chinese Academy of Sciences for their suggestions on this study. Our study was funded by National Key Research and Development Program of Ministry of Science and Technology (2017YFC0505703); National Natural Science Foundation of China (41801222); Key Program of Frontier Science of the Chinese Academy of Sciences (QYZDB-SSW-DQC012); Fujian Foreign Cooperation Funding (2019I0031).

Author contributions All authors contributed to the study conception and design. CC and JL: Material preparation, data collection and clean were performed. YL: Data analysis was performed. YL and WC: The first draft of the manuscript was written, and all authors commented on previous versions of the manuscript. All authors read and approved the final manuscript.

Conflict of interest The authors declare that they have no conflict of interest.

References

Augiseau V, Barles S (2017) Studying construction materials flows and stock: a review resources. Conserv Recycl 123:153–164.

Bailey RM (2011) Spatial and temporal signatures of fragility and threshold proximity in modelled semi-arid vegetation. Proc R Soc B 278:1064–1071.

Bechle MJ, Millet DB, Marshall JD (2011) Effects of Income and Urban Form on Urban NO2: global evidence from satellites. Environ Sci Technol 45:4914–4919.

Bereitschaft B, Debbage K (2013) Urban form, air pollution, and CO2 emissions in large U.S. Metrop Areas Prof Geogr 65:612–635.

Cao Q, Liu Y, Georgescu M, Wu J (2020) Impacts of landscape changes on local and regional climate: a systematic review. Landscape Ecol 35:1269–1290.

Che M, Du P, Gamba P (2018) 2- and 3-D urban change detection with quad-PolSAR data . IEEE Geosci Remote Sens Lett 15:68–72.

Chen Z, Xu B, Devereux B (2014) Urban landscape pattern analysis based on 3D landscape models. Appl Geogr 55:82–91.

Costanza R, d'Arge R, de Groot R, Farber S, Grasso M, Hannon B, Limburg K, Naeem S, O'Neill RV, Paruelo J, Raskin RG, Sutton P, van den Belt M (1997) The value of the world's ecosystem services and natural capital. Nature 387:253–260

Costanza JK, Riitters K, Vogt P, Wickham J (2019) Describing and analyzing landscape patterns: where are we now, and where are we going? Landscape Ecol 34:2049–2055.

Cumming G (2011) Spatial resilience: integrating landscape ecology, resilience, and sustainability. Landscape Ecol 26:899–909.

Davis AY, Jung J, Pijanowski BC, Minor ES (2016) Combined vegetation volume and “greenness” affect urban air temperature. Appl Geogr 71:106–114.

Ewing R, Pendall R, Chen D (2002) Measuring sprawl and its impact. Cornell University, Washington, DC

Ewing R, Schieber RA, Zegeer CV (2003) Urban sprawl as a risk factor in motor vehicle occupant and pedestrian fatalities. Am J Public Health 93:1541–1545.

Ewing R, Rong F (2008) The impact of urban form on U.S. residential energy use. Hous Policy Debate 19:1–30.

Fahrig L (2003) Effects of habitat fragmentation on biodiversity. Annu Rev Ecol Evol Syst 34:487–515

Forman RTT (1995) Some general principles of landscape and regional ecology. Landscape Ecol 10:133–142.

Frank S, Fürst C, Koschke L, Makeschin F (2012) A contribution towards a transfer of the ecosystem service concept to landscape planning using landscape metrics. Ecol Indic 21:30–38.

Galster G, Hanson R, Ratcliffe MR, Wolman H, Coleman S, Freihage J (2001) Wrestling sprawl to the ground: defining and measuring an elusive concept. Hous Policy Debate 12:681–717.

Hang J, Li Y, Sandberg M, Buccolieri R, Di Sabatino S (2012) The influence of building height variability on pollutant dispersion and pedestrian ventilation in idealized high-rise urban areas. Build Environ 56:346–360.

Hao R, Yu D, Liu Y, Liu Y, Qiao J, Wang X, Du J (2017) Impacts of changes in climate and landscape pattern on ecosystem services. Sci Total Environ 579:718–728.

Kedron P, Zhao Y, Frazier AE (2019) Three dimensional (3D) spatial metrics for objects. Landscape Ecol. https://doi.org/10.1007/s10980-019-00861-4

Li C, Li J, Wu J (2013a) Quantifying the speed, growth modes, and landscape pattern changes of urbanization: a hierarchical patch dynamics approach. Landscape Ecol 28:1875–1888.

Li J, Li C, Zhu F, Song C, Wu J (2013b) Spatiotemporal pattern of urbanization in Shanghai, China between 1989 and 2005. Landscape Ecol 28:1545–1565.

Liu M, Hu Y-M, Li C-L (2017a) Landscape metrics for three-dimensional urban building pattern recognition. Appl Geogr 87:66–72.

Liu Y, Wu J, Yu D (2017) Characterizing spatiotemporal patterns of air pollution in China: a multiscale landscape approach. Ecol Indic 76:344–356.

Liu Y, Wu J, Yu D (2018) Disentangling the complex effects of socioeconomic, climatic, and urban form factors on air pollution: a case study of China. Sustainability 10:776.

Liu Y, Wu J, Yu D, Hao R (2018) Understanding the patterns and drivers of air pollution on multiple time scales: the case of northern. China Environ Manag 61:1048–1061.

Liu Y, Wu J, Yu D, Ma Q (2018) The relationship between urban form and air pollution depends on seasonality and city size Environmental. Sci Pollut Res 25:15554–15567.

Luck M, Wu J (2002) A gradient analysis of urban landscape pattern: a case study from the Phoenix metropolitan region, Arizona, USA. Landscape Ecol 17:327–339.

Ludwig JA, Wilcox BP, Breshears DD, Tongway DJ, Anton CI (2005) Vegetation patches and runoff-erosion as interacting ecohydrological processes in semiarid. Landscape Ecol 86:288–297

McGarigal K, Cushman SA, Ene E (2012) FRAGSTATS v4: spatial pattern analysis program for categorical and continuous maps. In: Computer software program produced by the authors at the University of Massachusetts, Amherst

Metzger MJ, Rounsevell MDA, Acosta-Michlik L, Leemans R, Schröter D (2006) The vulnerability of ecosystem services to land use change. Agr Ecosyst Environ 114:69–85.

O’Neill RV, Krummel JR, Gardner RH, Sugihara G, Jackson B, DeAngelis DL, Milne BT, Turner MG, Zygmunt B, Christensen SW, Dale VH, Graham RL (1988) Indices of landscape pattern. Landscape Ecol 1:153–162

Pauliuk S, Müller DB (2014) The role of in-use stocks in the social metabolism and in climate change mitigation. Glob Environ Change 24:132–142.

Perera NGR, Emmanuel R (2018) A “Local Climate Zone” based approach to urban planning in Colombo. Sri Lanka Urban Clim 23:188–203.

Peterson GD (2002) Estimating resilience across landscapes. Conserv Ecol 6:17

Priyadarsini R, Hien WN, Wai David CK (2008) Microclimatic modeling of the urban thermal environment of Singapore to mitigate urban heat island. Sol Energy 82:727–745.

Reis JP, Silva EA, Pinho P (2016) Spatial metrics to study urban patterns in growing and shrinking cities. Urban Geogr 37:246–271.

Song Y, Knaap G-J (2004) Measuring urban form: is Portland winning the war on sprawl? J Am Plann Assoc 70:210–225.

Stewart ID, Oke TR (2012) Local climate zones for urban temperature studies B. AM Meteorol Soc 93:1879–1900.

Termorshuizen J, Opdam P (2009) Landscape services as a bridge between landscape ecology and sustainable development. Landscape Ecol 24:1037–1052.

Thacker S, Adshead D, Fay M, Hallegatte S, Harvey M, Meller H, O’Regan N, Rozenberg J, Watkins G, Hall JW (2019) Infrastructure for sustainable development. Nat Sustain 2:234–331

Tian Y, Zhou W, Qian Y, Zheng Z, Yan J (2019) The effect of urban 2D and 3D morphology on air temperature in residential neighborhoods. Landscape Ecol. https://doi.org/10.1007/s10980-019-00834-7

Tsai Y-H (2005) Quantifying urban form: compactness versus ‘sprawl’. Urban Stud 42:141–161.

Turner W, Spector S, Gardiner N, Fladeland M, Sterling E, Steininger M (2003) Remote sensing for biodiversity science and conservation . Trends Ecol Evol 18:306–314.

Wong MS, Nichol JE, To PH, Wang J (2010) A simple method for designation of urban ventilation corridors and its application to urban heat island analysis. Build Environ 45:1880–1889.

Wu J, David JL (2002) A spatially explicit hierarchical approach to modeling complex ecological systems: theory and applications. Ecol Model 153:7–26.

Wu J, Levin SA (1994) A spatial patch dynamic modeling approach to pattern and process in an annual. Grassland Ecol Monogr 64:447–464.

Wu J, Levin SA (1997) A patch-based spatial modeling approach: conceptual framework and simulation scheme. Ecol Model 101:325–346.

Wu J, Jenerette GD, Buyantuyev A, Redman CL (2011) Quantifying spatiotemporal patterns of urbanization: the case of the two fastest growing metropolitan regions in the United. States Ecol Complex 8:1–8.

Wu J (2013) Landscape sustainability science: ecosystem services and human well-being in changing landscapes. Landscape Ecol 28:999–1023.

Wu Q, Guo F, Li H, Kang J (2017) Measuring landscape pattern in three dimensional space. Landscape Urban Plan 167:49–59.

Xi FF, Davis SJ, Ciais P, Crawford-Brown D, Guan D, Pade C, Shi T, Syddall M, Lv J, Ji L, Bing L, Wang J, Wei W, Yang K-H, Lagerblad B, Galan I, Andrade C, Zhang Y, Liu Z (2016) Substantial global carbon uptake by cement carbonation. Nat Geosci 9:880

Yu D, Liu Y, Shi P, Wu J (2019) Projecting impacts of climate change on global terrestrial ecoregions. Ecol Indic 103:114–123.

Yuan C, Ng E, Norford LK (2014) Improving air quality in high-density cities by understanding the relationship between air pollutant dispersion and urban morphologies. Build Environ 71:245–258.

Zhang Y, Murray AT, Turner Ii BL (2017) Optimizing green space locations to reduce daytime and nighttime urban heat island effects in Phoenix Arizona. Landscape Urban Plan 165:162–171.

Zhang JJ, Fu MC, Chen J, Chu PP, Zhang CC (2018) Variations in mine subsidence-disturbed residential land price: case study of critical determinants and spatial relationships in the Nanhu Ecoregion of Tangshan, China. J Urban Plan Dev 144:16.

Zielinska-Dabkowska KM, Xavia K (2019) Protect our right to light. Nature 568:451–453

Zurlini G, Riitters K, Zaccarelli N, Petrosillo I, Jones KB, Rossi L (2006) Disturbance patterns in a socio-ecological system at multiple scales. Ecol Complex 3:119–128.